A MODEL FOR ANALYSIS OF THE TEMPERATURE FIELD

DOWNSTREAM OF A HEATED JET INJECTED INTO

AN ISOTHERMAL CROSSFLOW AT AN ANGLE OF 90°

V. L. Eriksen,

E. R. G. Eckert,

R. J. Goldstein

CASE FILE
COPY

HEAT TRANSFER LABORATORY

MECHANICAL ENGINEERING DEPARTMENT

UNIVERSITY OF MINNESOTA

SUMMARY REPORT

A MODEL FOR ANALYSIS OF THE TEMPERATURE FIELD
DOWNSTREAM OF A HEATED JET INJECTED INTO
AN ISOTHERMAL CROSSFLOW AT AN ANGLE OF 90°

by

V. L. Eriksen, E.R.G. Eckert, and R. J. Goldstein

prepared for

NATIONAL AERONAUTICS AND SPACE

ADMINISTRATION

July 1971

University of Minnesota
Institute of Technology
Department of Mechanical Engineering
Minneapolis, Minnesota 55455

ABSTRACT

The temperature distribution downstream of a heated jet entering an isothermal crossflow at an angle of 90° is predicted using two conduction models with energy sources above the point of injection, in one case a point source and in the second a line source. The models use effective turbulent diffusivities that are determined empirically from previous measurements. Temperatures predicted by the models are compared to experimental results.

NOMENCLATURE

c_p specific heat at constant pressure per unit mass

D   diameter of injection tube

k   thermal conductivity

M   blowing rate parameter, $\rho_2 U_2/\rho_\infty U_\infty$

$\dot{q}$ strength of line source per unit length

$\dot{Q}$ strength of energy source and enthalpy flow through injection hole; energy/time

T   temperature

T_{aw} adiabatic wall temperature

T_m maximum temperature of (y direction) profile

T_2 temperature of injected air

T_∞ mainstream temperature

U   velocity

U_2 average velocity of secondary flow

U_∞ mainstream velocity

X   distance downstream from center of injection hole, see Figure 1

X_o component of distance from center of injection hole to energy source in X direction

Y   distance normal to wall through which injected air flows, see Figure 1

Y_o component of distance from center of injection hole to energy source in Y direction

Z   lateral distance from center of injection hole, see Figure 1

Z_o component of distance from center of injection hole to energy source in Z direction

α molecular thermal diffusivity = $\dfrac{k}{\rho c_p}$

δ boundary layer thickness

ϵ turbulent thermal diffusivity

ϵ_ℓ turbulent thermal diffusivity for line source model

ϵ_p turbulent thermal diffusivity for point source model

$\bar{\epsilon}$ average turbulent thermal diffusivity

η film cooling effectiveness, defined by Equation 2

θ temperature difference, $T - T_\infty$

θ_m maximum temperature difference, $T_m - T_\infty$

θ_2 injection temperature difference, $T_2 - T_\infty$

ν kinematic viscosity

ρ density

ρ_2 density of injected air

ρ_∞ density of mainstream

A MODEL FOR ANALYSIS OF THE TEMPERATURE FIELD
DOWNSTREAM OF A HEATED JET INJECTED INTO
AN ISOTHERMAL CROSSFLOW AT AN ANGLE OF 90°

by

V. L. Eriksen, E.R.G. Eckert, and R. J. Goldstein

University of Minnesota

I. SUMMARY

The study described in this report is part of an
investigation into film cooling following ejection of a
secondary gas through discrete holes into a turbulent
boundary layer of air on a flat plate. Two models to predict
film cooled temperatures are described and their predictions
are compared to previous measurements.

The models are based on conduction solutions for a
point and a line source of energy moving in an infinite medium.
The influence of blowing rate is accounted for by positioning
the sources above the point of injection. The turbulent flow
characteristics are considered by replacing the molecular
thermal diffusivity as it appears in the conduction solution
by an effective average turbulent thermal diffusivity. This
effective turbulent diffusivity is evaluated by matching the
conduction solutions to experimental results for a heated
jet injected into an isothermal crossflow at an angle of 90°.

The point source model adequately predicts the temperature along the centerline downstream of injection but not at lateral positions. The line source model takes into account the finite width of the injection hole and is a better representation than the point source model for determining off-centerline temperature. It does not, however, predict centerline temperature quite as well as the point source model.

II. INTRODUCTION

Film cooling is used extensively in various modern devices. As a consequence, a large body of literature is concerned with the prediction of the effectiveness of this cooling method. It deals, however, almost exclusively with ejection of the coolant through openings which are uninterrupted in the direction normal to the main flow. This arrangement creates a temperature field in the fluid downstream of the openings which is two-dimensional, having the same characteristic in all planes normal to the film cooled surface and parallel to the main flow direction.

In various applications, design considerations require that the openings for the ejection of the coolant be interrupted or that they consist of rows of holes. That is, for instance, the case for the film cooling of gas turbine blades. In such an arrangement, the temperature field in the fluid downstream of the openings is three-dimensional and the temperature on

the film cooled surface is two-dimensional. The number of geometries in such an arrangement is almost unlimited because the shape of the openings, their mutual distance, and the direction in which the coolant is ejected can all vary; several rows at various positions along the flow direction may also be considered. The cooling effectiveness created by such an arrangement will depend on the dimensionless parameters describing the main flow as well as the flow of the coolant as it leaves the openings. A test program which covers these parameters becomes therefore very extensive. Predicting the film cooling performance would be simplified if the information could be restricted to average temperatures. Design calculations require, however, the knowledge of the complete temperature field at the film cooled surface. Under these circumstances it is desirable to have an analytical model available which describes the film cooling process at least qualitatively and which, in addition, can be used to interpolate between the test points. Such a model was suggested in reference 1 and proved in the meantime its usefulness for two-dimensional film cooling. An analogous model is described in reference 2 for three-dimensional film cooling. It replaces the ejection of the coolant through a hole by a point energy sink. With the additional assumption that the variation of the properties involved in the cooling process can be neglected, the law of super-position can be applied to the energy sink model and all possible coolant configurations--

like one row or several rows of holes or interrupted slots--
can be modeled by super-position of such point heat sinks.
It was shown in reference 2 that the energy sink model
approximates experimental results for normal ejection of air
through a circular hole into a turbulent air boundary layer
satisfactorily as long as the ratio of the mass velocity
with which the coolant leaves the opening to the mass velocity
of the mainstream is small. The present report proposes an
extension of this model which leads to an improved approximation
of the actual conditions for larger ratios of the mass velocities.
It also compares the predictions obtained with this model with
experimental results.

The study is specifically concerned with the configuration
shown in Figure 1. A jet of density ρ_2, temperature T_2, and
mean velocity U_2 enters a main flow of density ρ_∞, and mainstream
velocity U_∞. The angle between the axis of the entering jet
and the direction of the free stream does not appear as
parameter in the analysis. In the experiments to which the
analytical results will be compared it is 90°. The hole
through which the jet flows is flush with the surface that is
to be protected. A turbulent boundary layer of thickness δ
is present at the location of the hole. The wall downstream
of the hole is postulated to be adiabatic in the sense that the
heat flux from the fluid to the surface is zero. The adiabatic
wall temperature which this surface assumes is of interest
in itself and has also been demonstrated to be a useful

parameter for conditions in which a heat flux is generated
either by conduction into the wall or by radiation from the
wall surface.

It is well established that heat transfer relations have
the same form for the situations in which the fluid ejected
through the hole has a higher or lower temperature than the
mainstream fluid. The experiments to which the analysis in
this report will be compared have been performed with the
temperature T_2 larger than T_∞. Therefore, the analytical
models will, from here on, consider energy sources.

Temperatures in the flow field will be represented in
dimensionless form

$$\frac{\theta}{\theta_2} = \frac{T-T_\infty}{T_2-T_\infty} \tag{1}$$

The adiabatic wall temperatures are described by the film
cooling effectiveness

$$\eta = \frac{T_{aw}-T_\infty}{T_2-T_\infty} \tag{2}$$

The following parameters will be used to describe the temperature
distribution in the flow and the film cooling effectiveness:
The free stream Reynolds number, $Re_\infty = \frac{U_\infty D}{\nu}$, the mass velocity
ratio or blowing rate M ($M = \rho_2 U_2 / \rho_\infty U_\infty$), and the thickness δ
of the boundary layer approching the jet. The density ratio
ρ_2/ρ_∞ is specified as close to unity in the analysis and was
approximately 0.85 in the experiments, the results of which are
used in this paper.

III. POINT ENERGY SOURCE ABOVE THE CENTER OF INJECTION

Measurements of the temperature field downstream of the point of injection as well as flow visualization have demonstrated that the flow ejected from a hole into a mainstream separates from the surface when the blowing rate exceeds a certain value ($M \sim 0.4 - 0.5$). The model described in this section accounts for this fact in the way that a point energy source* is located some distance above the center of the secondary fluid injection hole (Figure 2a). In developing this model we start with an equation which describes the temperature distribution downstream of an energy source of strength $\dot{Q}$, located at X_0, Y_0, Z_0, with an infinite medium moving in steady uniform flow past the source in the positive X direction with velocity U_∞ (reference 3).

$$\theta(X,Y,Z) = \frac{\dot{Q} \exp\left\{-\frac{U_\infty}{2\alpha}\left[\left|\sqrt{(X-X_0)^2 + (Y-Y_0)^2 + (Z-Z_0)^2}\right| - (X-X_0)\right]\right\}}{4\pi k \sqrt{(X-X_0)^2 + (Y-Y_0)^2 + (Z-Z_0)^2}} \quad (3)$$

For the system shown in Figure 2(a), the source is located directly above the center of injection with $X_0 = 0$ and $Z_0 = 0$. Equation 3 thus simplifies to

$$\theta(X,Y,Z) = \frac{\dot{Q} \exp\left\{-\frac{U_\infty}{2\alpha}\left[\left|\sqrt{X^2 + (Y-Y_0)^2 + Z^2}\right| - X\right]\right\}}{4\pi k \sqrt{X^2 + (Y-Y_0)^2 + Z^2}} \quad (4)$$

*Although the term "heat source" (or sink) is often used in conduction models, "energy source" is actually a more general term.

-6-

If the calculation is restricted to the region where X
is large compared to $Y-Y_o$ and Z, then

$$\sqrt{X^2 + (Y-Y_o)^2 + Z^2} \simeq X$$

and

$$\sqrt{X^2 + (Y-Y_o)^2 + Z^2} - X \simeq \frac{(Y-Y_o)^2}{2X} + \frac{Z^2}{2X}$$

for $X > 0$. The equation for the temperature distribution
in this region is now

$$\theta(X,Y,Z) = \frac{\dot{Q} \exp\left\{- \frac{U_\infty}{4\alpha X}\left[(Y-Y_o)^2 + Z^2\right]\right\}}{4\pi k X} \tag{5}$$

The strength of the point source is equated to the enthalpy
transport $\dot{Q}$ due to mass injection

$$\dot{Q} = \rho_\infty U_\infty M \frac{\pi D^2}{4} \bar{c}_{p_2} \theta_2 \tag{6}$$

Assuming $c_{p_2} = c_{p_\infty}$, equation (5) can now be written

$$\frac{\theta(X,Y,Z)}{\theta_2} = \frac{MU_\infty D}{16\alpha\frac{X}{D}} \exp\left\{- \frac{U_\infty D}{4\alpha\frac{X}{D}}\left[\left(\frac{Y-Y_o}{D}\right)^2 + \left(\frac{Z}{D}\right)^2\right]\right\} \tag{7}$$

Equation 7 has to be adapted to the film cooling process
in which the secondary fluid is injected into a turbulent
boundary layer. This can be done to a first approximation
if the thermal diffusivity α is replaced by a turbulent

diffusivity ϵ_p. This neglects the local variation of the thermal diffusivity in the boundary layer and assumes a homogeneous and isotropic field of turbulence. Wieghardt (Reference 4) and Malhotra and Cermak (Reference 5) have investigated experimentally heat and mass transfer respectively from a point heat and mass source into a turbulent boundary layer. They use relations similar to Equation 5 to correlate their experimental results.

There is another adjustment which has to be made so that the energy source model matches the boundary conditions on an adiabatic wall. This can be done by the method of images. For this purpose, the solution for another source at $Y = -Y_o$ is added to Equation 7. This results in the equation

$$\frac{\theta(X,Y,Z)}{\theta_2} = \frac{MU_\infty D}{16\epsilon_p \frac{X}{D}} \exp\left\{-\frac{U_\infty D}{4\epsilon_p \frac{X}{D}}\left[\left(\frac{Y-Y_o}{D}\right)^2 + \left(\frac{Z}{D}\right)^2\right]\right\} +$$

$$\frac{MU_\infty D}{16\epsilon_p \frac{X}{D}} \exp\left\{-\frac{U_\infty D}{4\epsilon_p \frac{X}{D}}\left[\left(\frac{Y+Y_o}{D}\right)^2 + \left(\frac{Z}{D}\right)^2\right]\right\} \qquad (8)$$

To use Equation 8, the distance Y_o at which the heat source is located above the surface and the turbulent diffusivity ϵ_p have to be determined. The following procedure is proposed: determine the average value, Y_m, of the distance to the temperature maximum above the surface (see Figure 1) for those

values X and Y for which measurements are available within the range for which interpolation is desired. The arithmetic mean of these values Y_m is interpreted as Y_o. In general, measured values of the film cooling effectiveness are used to determine the turbulent diffusivity ε_p. The film cooling effectiveness η is equal to the temperature ratio θ/θ_2 for $Y = 0$. Rearranging Equation 8 yields for this condition

$$\varepsilon_p = \frac{MU_\infty D}{8\eta(X,Z)\frac{X}{D}} \exp\left\{ - \frac{U_\infty D}{4\varepsilon_p\frac{X}{D}}\left[\left(\frac{Y_o}{D}\right)^2 + \left(\frac{Z}{D}\right)^2\right]\right\} \qquad (9)$$

This equation must be solved by iteration because the turbulent diffusivity appears on both sides. It is proposed to calculate turbulent diffusivities with Equation 9 for those locations for which adiabatic wall temperature data are available within the range selected for interpolation, to determine the arithmetic mean of these diffusivities, and to use the mean in Equation 8. Although single values of $\overline{\varepsilon}_p$ and Y_o are used to predict η over the whole test surface, local values could be determined for interpolation.

For very large blowing rates, the values of the film cooling effectiveness are small and generally available with moderate accuracy only. An alternative procedure for determining ε_p can then be based on the maximum temperature T_m (Figure 1). Evaluating Equation 8 at that location leads to

$$\epsilon_p = \frac{MU_\infty D}{16\frac{\theta}{\theta}_2\bigg|_m\frac{X}{D}}\left\{1 + \exp\left[-\frac{U_\infty D}{\epsilon_p\frac{X}{D}}\left(\frac{Y_m}{D}\right)^2\right]\right\} \tag{10}$$

which can be used in the same way as Equation 9 to obtain
an average value of the turbulent diffusivity for insertion
back into Equation 8, which will be used as an interpolation
formula.

IV. LINE HEAT SOURCE ABOVE THE POINT OF INJECTION

If the model is used to simulate injection of a secondary
fluid through a hole of finite diameter, it can be suspected
and it is verified by the calculations in the latter part of
this report that the point heat source underestimates the
lateral spreading of the temperature. This raises the
question whether the analytical model can be improved without
making the analysis too unwieldy and suggests the following
extension. A line source with a length D extending in the
lateral direction Z is arranged at the location of the hole
as shown in Figure 2b. The strength $\dot{q}$ per unit length of
the line source is postulated constant. The total strength
of the line source has to be the same as the enthalpy input
$\dot{Q}$ due to mass injection. Thus, from Equation 6

$$\dot{Q} = \rho_\infty U_\infty M\frac{\pi D^2}{4}c_{p2}\theta_2 = \int_{-.5D}^{.5D}\dot{q}\,dZ = \dot{q}D \tag{11}$$

-10-

The equation for the temperature distribution downstream of the model is derived by considering Equation 5 for a point source ($\dot{q}dZ_o$) that is located at Y_o, Z_o.

$$\theta(X,Y,Z) = \frac{\dot{q}dZ_o}{4\pi kX} \exp\left\{- \frac{U_\infty}{4\alpha X}\left[(Y-Y_o)^2 + (Z-Z_o)^2\right]\right\} \qquad (12)$$

The strength $\dot{q}$ is obtained from Equation 11 and the temperature distribution downstream of a line source is then obtained by integration over the length of the source

$$\theta(X,Y,Z) = \int_{-.5}^{.5} \frac{\rho_\infty U_\infty MDC_{p2}\theta_2}{16k\frac{X}{D}} \exp\left\{- \frac{U_\infty D}{4\alpha\frac{X}{D}}\left[\left(\frac{Y-Y_o}{D}\right)^2 +\left(\frac{Z-Z_o}{D}\right)^2\right]\right\}d\left(\frac{Z_o}{D}\right) \quad (13)$$

Assuming $c_{p2} = c_{p\infty}$ and carrying out the integration yields,

$$\frac{\theta(X,Y,Z)}{\theta_2} = \left\{\frac{M\sqrt{\pi}}{16}\sqrt{\frac{U_\infty D}{\alpha\frac{X}{D}}} \exp\left[- \frac{U_\infty D}{4\alpha\frac{X}{D}}\left(\frac{Y-Y_o}{D}\right)^2\right]\right\}x$$

$$\left\{\mathrm{erf}\left[\frac{1}{2}\sqrt{\frac{U_\infty D}{\alpha\frac{X}{D}}}\left(\frac{Z}{D} + 0.5\right)\right]- \mathrm{erf}\left[\frac{1}{2}\sqrt{\frac{U_\infty D}{\alpha\frac{X}{D}}}\left(\frac{Z}{D} - 0.5\right)\right]\right\}(14)$$

The adiabatic boundary condition at the wall is satisfied by the addition of an image line source at $Y = -Y_o$ and the turbulent flow characteristics are considered by replacing the molecular thermal diffusivity with a constant, isotropic, turbulent diffusivity ε_ℓ. The resulting expression for the temperature distribution in the turbulent flow above the adiabatic wall and downstream of the line energy source is

$$\frac{\theta(X,Y,Z)}{\theta_2} = \frac{M\sqrt{\pi}}{16}\sqrt{\frac{U_\infty D}{\varepsilon_\ell \frac{X}{D}}}\left\{\exp\left[-\frac{U_\infty D}{4\varepsilon_\ell \frac{X}{D}}\left(\frac{Y-Y_0}{D}\right)^2\right] + \exp\left[-\frac{U_\infty D}{4\varepsilon_\ell \frac{X}{D}}\left(\frac{Y+Y_0}{D}\right)^2\right]\right\}x$$

$$\left\{\text{erf}\left[\frac{1}{2}\sqrt{\frac{U_\infty D}{\varepsilon_\ell \frac{X}{D}}}\left(\frac{Z}{D}+0.5\right)\right] - \text{erf}\left[\frac{1}{2}\sqrt{\frac{U_\infty D}{\varepsilon_\ell \frac{X}{D}}}\left(\frac{Z}{D}-0.5\right)\right]\right\} \quad (15)$$

The distance Y_0 of the line heat source from the wall and
the turbulent diffusivity ε_ℓ can be determined in the same
way as for the point heat source to use in the interpolation
formula (Equation 15).

V. COMPARISON WITH EXPERIMENTAL RESULTS

The Point Source Model

It is important to investigate to what degree the
trends in the temperature field and the film cooling effec-
tiveness obtained by the proposed models agree with the results
of measurements. Such a comparison will be presented in
this section for the point energy source model and in the
following section for the line energy source model. Extensive
experimental results for film cooling effectiveness with
injection through a circular hole are described in Reference 6
and results describing the temperature field in the fluid
in Reference 7. The data for normal injection contained
therein will be used in the present comparison.

The temperature profiles of Reference 7 were used to determine Y_o. The distance Y_m from the peak of the temperature profile (see Figure 1) to the wall was obtained from the reference for profiles at X/D = 3.56, 5.48, and 10.57, and Z/D = 0.0, 0.25, and 0.50. The arithmetic average of these values at a given M is assumed to be Y_o. The result is presented in Figure 3. It can be observed that the distance at which the source has to be located above the wall increases with blowing rate due to increased jet penetration. Effectiveness data from Reference 6 were used to determine ϵ_p. For sets of values of M and U_∞, Reference 6 gives an array of effectiveness values in the area $1.3 < X/D < 42$ and $0.0 \leq Z/D \leq 1.5$. Equation 9 was applied to each point in this area. The values of Y_o/D needed for the calculation were taken from Figure 3. Since the model was formulated for the region $X/D \gg Z/D$, the iteration scheme to solve Equation 9 did not converge in the area where X/D is not large compared to Z/D. In the area where the model holds, a value of ϵ_p was calculated at each point $(X/D, Z/D)$. The arithmetic mean of these values (about 100 points) was then calculated. These values of $\overline{\epsilon}_p$ for each value of M and U_∞ are shown on Figure 4.

At high values of the blowing rate, the jet penetrates into the free stream and has little influence on the wall temperature. Equation 10 was then used to obtain ϵ_p from each of the centerline temperature profiles in Reference 7

at four axial locations (X/D = 1.87, 3.56, 5.48, and 10.57) where profiles were measured for each value of M and U_∞. Values of $\bar{\epsilon}_p$ calculated with this procedure are also shown in Figure 4.

The effective turbulent diffusivity is seen to increase with the blowing rate M. It can be observed that at the same values of U_∞ and M (M = 0.1 and U_∞ = 60.6 m/s or M = 0.5 and U_∞=30.3 m/s) agreement between the diffusivities obtained by the two methods is quite good. Figure 5 greatly reduces the dependence on free stream velocity by presenting $\bar{\epsilon}_p$ in dimensionless form. The quantity $\bar{\epsilon}_p/U_\infty D$ used in this figure is the inverse of the Peclet number with the molecular thermal diffusivity replaced by the effective turbulent diffusivity.

Using the values of Y_o/D and $\bar{\epsilon}_p$ from Figures 3 and 4 and Equation 8, some temperature profiles were predicted and compared with measured profiles from Reference 7. The experimental points and calculated lines are shown for blowing rates M = 0.10, 0.51, 0.99, and 2.01 on Figures 6-9 respectively. The profiles are located in the centerline plane (Z/D = 0) and at four different downstream locations.

Positioning the source a distance Y_o/D above the point of injection has the effect of moving the peak of the temperature profile away from the wall and into the flow at the higher blowing rates. Agreement between the model's predictions

and the experimental data is good at the low blowing rates, as was already demonstrated in Reference 2, and at the downstream stations for the higher blowing rates.

Predicted and measured values of the film cooling effectiveness at blowing rates M = 0.10, 0.51, and 1.00 are shown in Figures 10-12. The blowing rate M = 2.0 is not included since both measured and predicted values of η are very small. The experimental values of the film cooling effectiveness are taken from Reference 6. The lines were calculated with Equation 8 using values of Y_0/D from Figure 3 and the effective turbulent diffusivity for the point source model from Figure 4. The dependence of the film cooling effectiveness upon the distance X/D downstream of injection is shown at several lateral positions in the lower part of each figure. The curves exhibit the desired shape except for the region immediately downstream of injection, and agreement between the model and experimental results is good along the centerline (Z/D = 0.0). Better agreement close to the injection location might be obtained by removing the assumption that X is large (made following Equation 4) and using the resulting equation which would replace Equation 8. Agreement is not as good at locations off the centerline. The predicted values of the film cooling effectiveness are usually low at these lateral positions.

The plots in the upper right corner of each figure, where the film cooling effectiveness is shown as a function of the lateral position Z/D at several downstream locations, point this difference out more clearly. The temperature distribution resulting from the point source is too narrow. This is obviously a consequence of the fact that the energy released through the hole in the experiments is distributed over an area of one diameter width, whereas the point energy source has no width at X/D = 0.

In summary, it can be concluded that a single value of the distance Y_o and of the turbulent diffusivity $\bar{\varepsilon}_p$ over the area used in this section describes the trends in the development of the temperature field and in the effectiveness qualitatively quite well. If a more accurate quantitative prediction is desired, then the parameters Y_o and ε_p have to be determined over a narrower area. Equation 8 with these values then constitutes an interpolation formula for the respective area.

The Line Source Model

As with point source model, it is necessary to determine the distance the source lies above the wall and the effective turbulent diffusivity before the model can be applied. The distance Y_o/D from the line source to the wall is assumed to be identical to that used for the point source (see Figure 3).

Data from Reference 6 were used to obtain the diffusivity $\bar{\epsilon}_\ell$
and the procedure was the same as that used for a point source,
only now Equation 15 was applied. Again, the convergence
scheme did not converge in the area where X/D is not large
compared to Z/D. The numerical average of the individual
values of ϵ_ℓ (about 100 points) was calculated in the area
where the model holds. These values of $\bar{\epsilon}_\ell$ are shown for
each value of M and U_∞ in Figure 13. At high values of the
blowing rate, it was again necessary to use maximum temperatures
measured in the flow to determine ϵ_ℓ from Equation 15. The
results of this calculation are included in Figure 13. Agree-
ment between the results of the two methods of determining
$\bar{\epsilon}_\ell$ at the same values of U_∞ and M is again good. The values
of the effective turbulent diffusivity $\bar{\epsilon}_\ell$ for the line source
model are slightly less than the values $\bar{\epsilon}_p$ for the point
source model. Figure 14 shows the inverse of the Peclet
number based on the effective turbulent diffusivity $\bar{\epsilon}_\ell$.

Using values of Y_o/D from Figure 3 and $\bar{\epsilon}_\ell$ from Figure 13,
the line heat source model was used to predict some of the
experimental temperature profiles from Reference 7. The
experimental points and calculated lines are shown on Figures
15-18 for blowing rates M = 0.10, 0.51, 0.99, and 2.01. The
profiles are located in the plane Z/D = 0 and at four different
downstream locations X/D. The calculated profiles have the
same shape as those that were calculated for the point source

-17-

since the functional form of the equations for the point
source (Equation 8) and line source (Equation 15) is the
same with respect to Y/D. Because the values of $\bar{\epsilon}_\ell$ are
lower than the values of $\bar{\epsilon}_p$, the calculated temperature
profiles (at Z/D = 0) for the line source do not agree as
well with the experimental profiles as those for the point
source at blowing rates M = 0.10 and 0.51. There is only a
slight difference between the two sets of calculated profiles
at the blowing rates M = 0.99 and 2.01.

Figures 19-21 present comparisons of experimental values
of the film cooling effectiveness of Reference 6 and values
predicted by the line source model at blowing rates M = 0.10,
0.51, and 1.00. The blowing rate M = 2.0 is not included
since both measured and predicted values of the film cooling
effectiveness are very small. Again values of Y_o/D from
Figure 3 and values of $\bar{\epsilon}_\ell$ from Figure 13 were used in the
calculation. There is some improvement in the off-centerline
values of the film cooling effectiveness predicted by the
line source model over those predicted by the point source
model. It is, however, questionable whether the improvement
warrants the use of the line wource model over the point source.

Various other adjustments of the energy source model
suggest themselves. Better agreement on lateral spreading
may be obtainable by a model consisting of two point sources
arranged at a distance D apart at X = 0 and Z = $\pm$ D/2. The

local variation of the turbulent diffusivity in the boundary
layer could be included by an empirical adjustment of Equation 8,
leading to equations similar to those in References 4 and 5.
One might also try to use the centerline of the actual jet (the
location of the maximum temperature T_m) for the centerline of
the temperature field resulting from the energy source.
Effects of the boundary layer thickness at the point of injected
fluid would then enter the model through their effect on the
trajectory of the jet. This, however, would require knowledge
of the jet centerline which generally is not available. It
is suspected that all these adjustments will not lead to
an essential improvement of the results obtained with the
various models.

Some effort was also spent in developing an empirical
equation by statistically requiring best agreement of such
an equation with the experimental results. Even expressions
of a fairly complicated nature could not represent these
results with a higher accuracy than the point source model.
This is obviously due to the complicated nature of the
interaction and of the mixing of the secondary fluid jet with
the turbulent boundary layer at larger values of the blowing
parameter M.

It is, therefore, felt that the best procedure for
design calculations is to use the experimental information on
film cooling parameters as it is contained in the literature and

as it will become available in the future and to interpolate
between the experimental data by the equations derived from
the point heat source model with values of Y_o and ϵ_p
determined in the area of interpolation. For rows of holes
or for interrupted slots, use should be made of the super-
position principle to adjust the interpolation formula to
this condition, though care must be taken due to the inter-
action of jets, particularly far downstream.

VI. CONCLUSIONS

1. The point energy source model of Reference 2 can be
   adapted to describe film cooling with ejection through a
   circular hole at large blowing rates by locating the
   source some distance above the film cooled surface.

2. Use of a line energy source with a length equal to the
   diameter of the hole somewhat improves the agreement
   between the temperature field and effectiveness calculated
   with the model and experimental results obtained for
   ejection of the secondary fluid through a hole.

3. For closer quantitative agreement it is suggested that the
   relations obtained from the energy source models be used
   as interpolation formulas upon determining the distance
   of the source above the wall and the turbulent diffusivity
   from experimental information in the area close to the
   desired location.

ACKNOWLEDGMENTS

BIBLIOGRAPHY

1. E.R.G. Eckert, "Transpiration and Film Cooling," in Heat Transfer Symposium, University of Michigan Press, 1953.

2. J.W. Ramsey, R.J. Goldstein, and E.R.G. Eckert, "A Model for Analysis of the Temperature Distriubtion with Injection of a Heated Jet into an Isothermal Flow," Heat Transfer 1970, Elsevier Publishing Co., Amsterdam, Netherlands, 1970.

3. H.S. Carslaw and J.C. Jaeger, Conduction of Heat in Solids, Oxford University Press, London, pp. 266-267, 1959.

4. K. Wieghardt, "Uber Ausbreitungsvorgänge in Turbulenten Reibungsshichten," A. Agnew, Math. Mech. 28 No. 11-12, pp. 346-355, 1948.

5. R.C. Malhotra and J.E. Cermak, "Mass Diffusion in Neutral and Unstably Stratified Boundary-Layer Flows," Int. J. Heat Mass Transfer, 7, pp. 169-186, 1964.

6. R.J. Goldstein, E.R.G. Eckert, and J.W. Ramsey, "Film Cooling with Injection Through a Circular Hole," NASA Cr-54604, May, 1968; (Trans. ASME, Series A, Vol 90

7. J.W. Ramsey, and R.J. Goldstein, "Interaction of a Heated Jet with a Deflecting Stream," NASA CR-72613, April, 1970; (University of Minnesota, HTL TR No. 92).
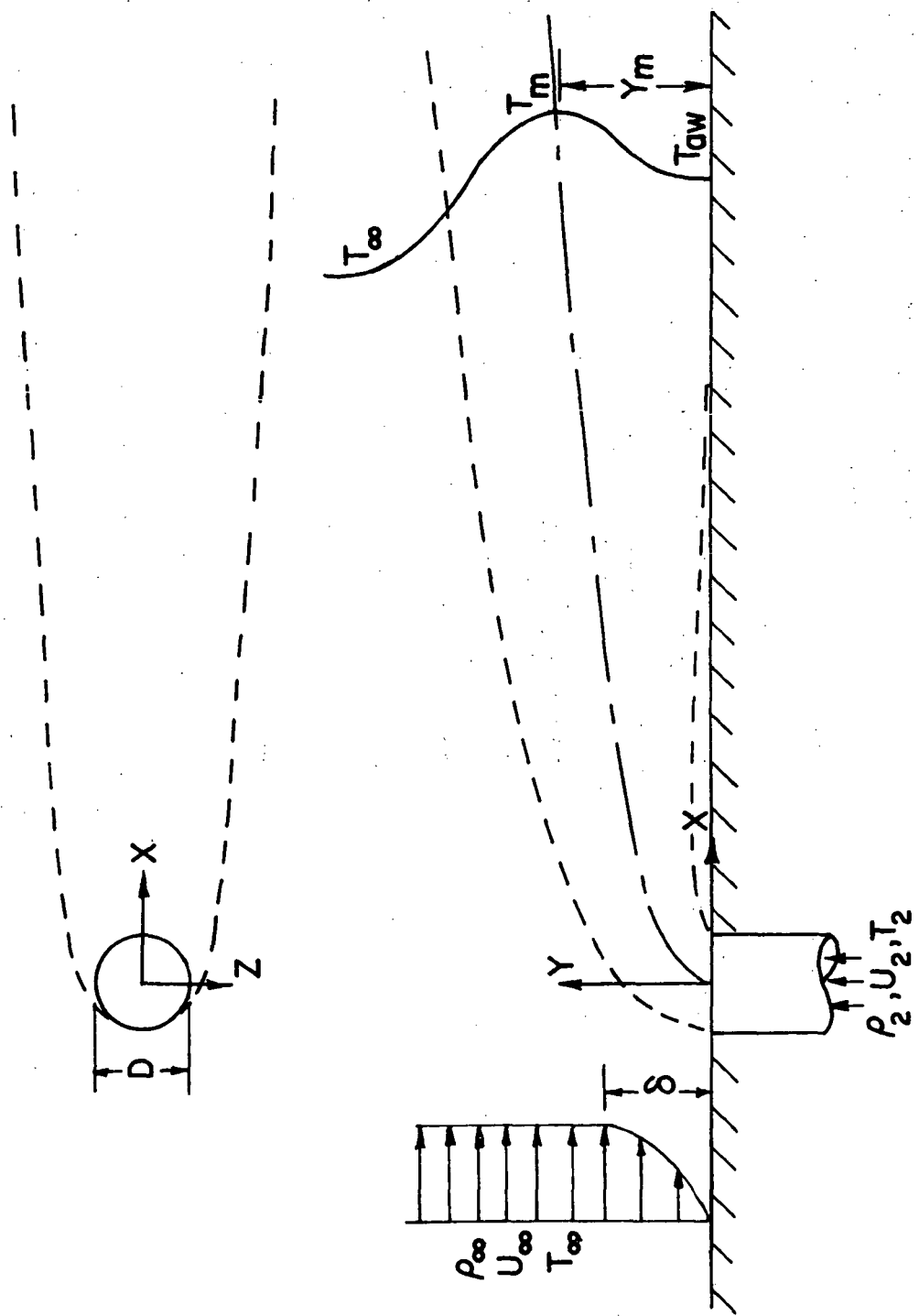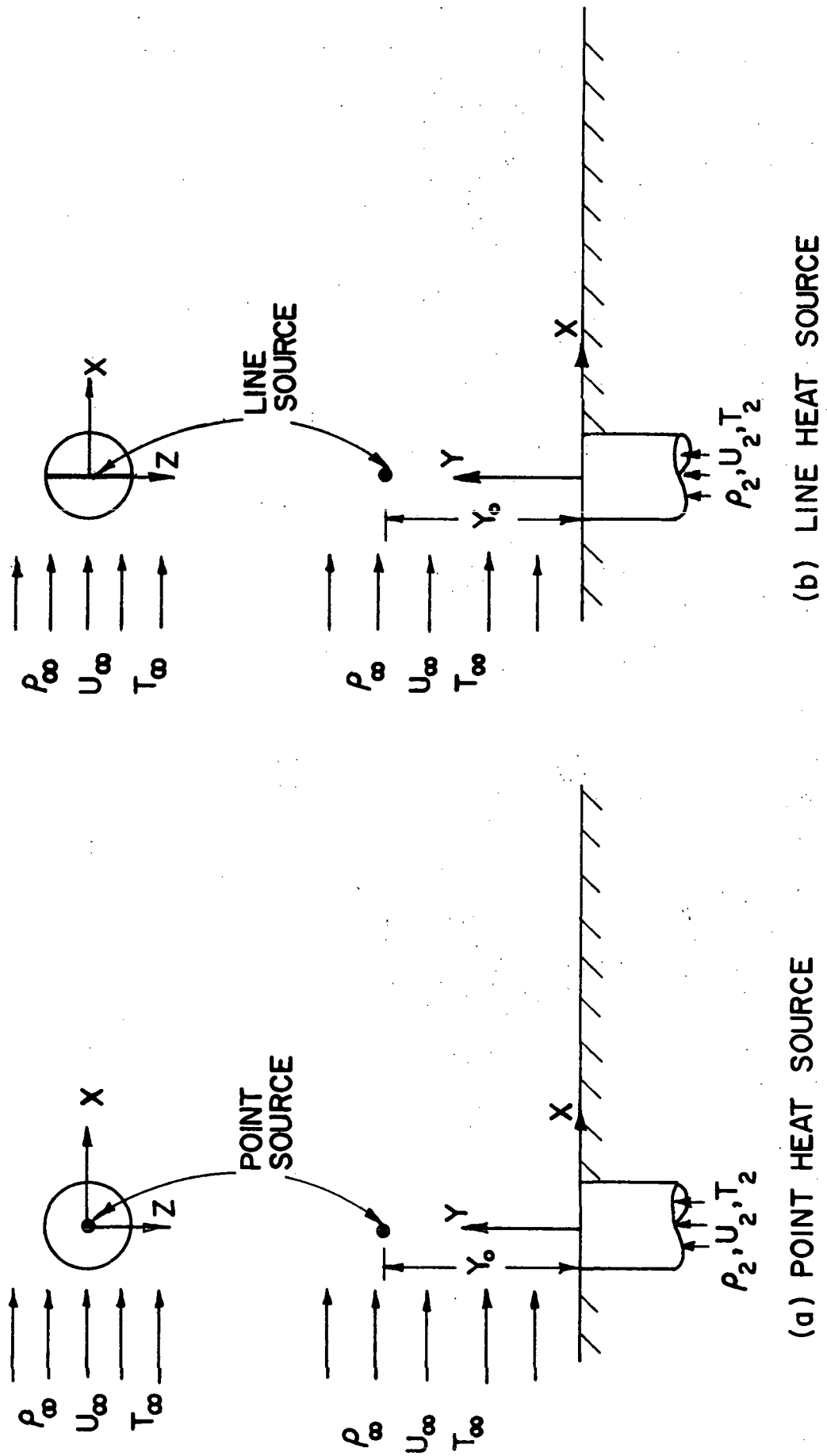
Figure 1 - Circular jet injected normal to a crossflow

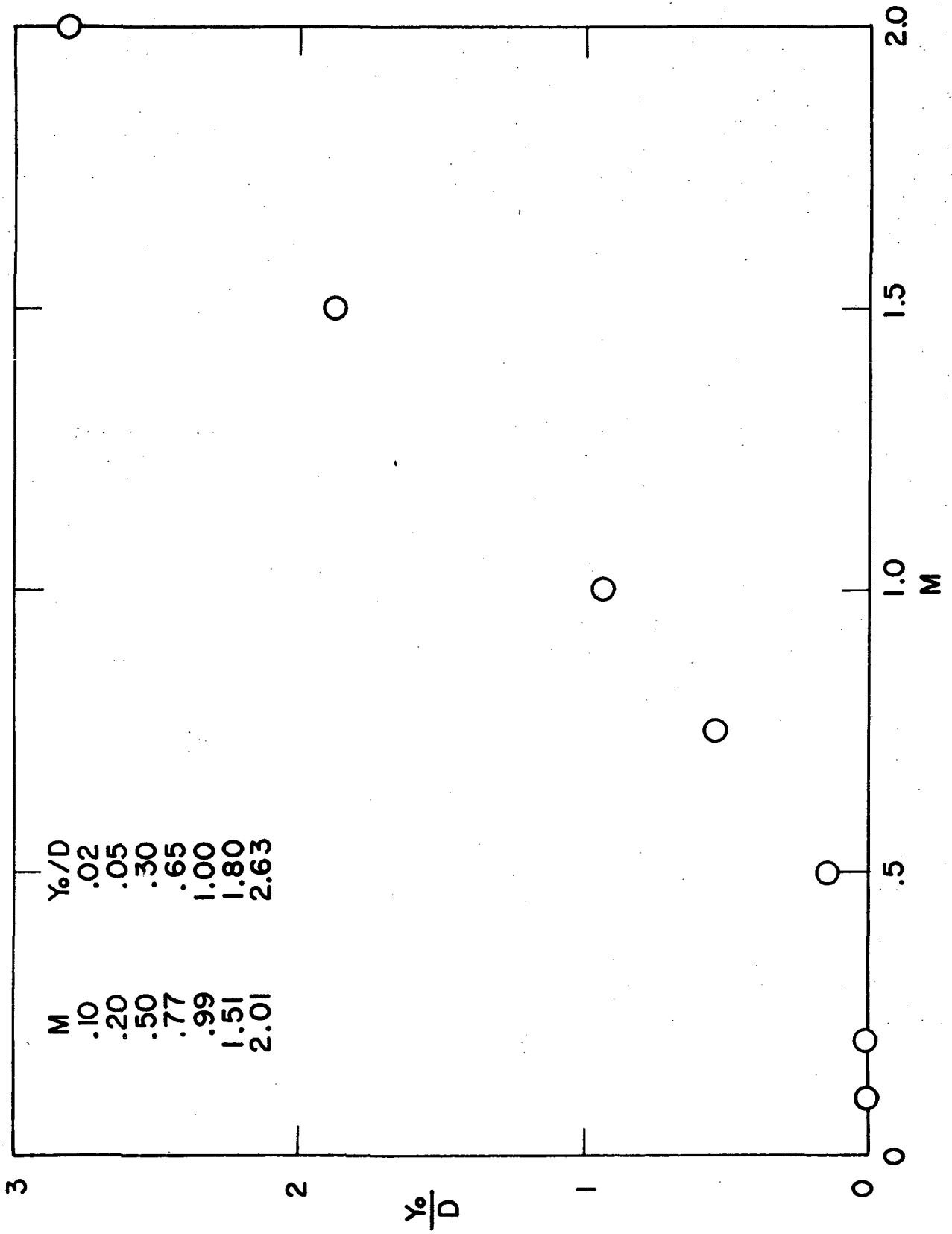Figure 2 - Location of point and line source models in the crossflow

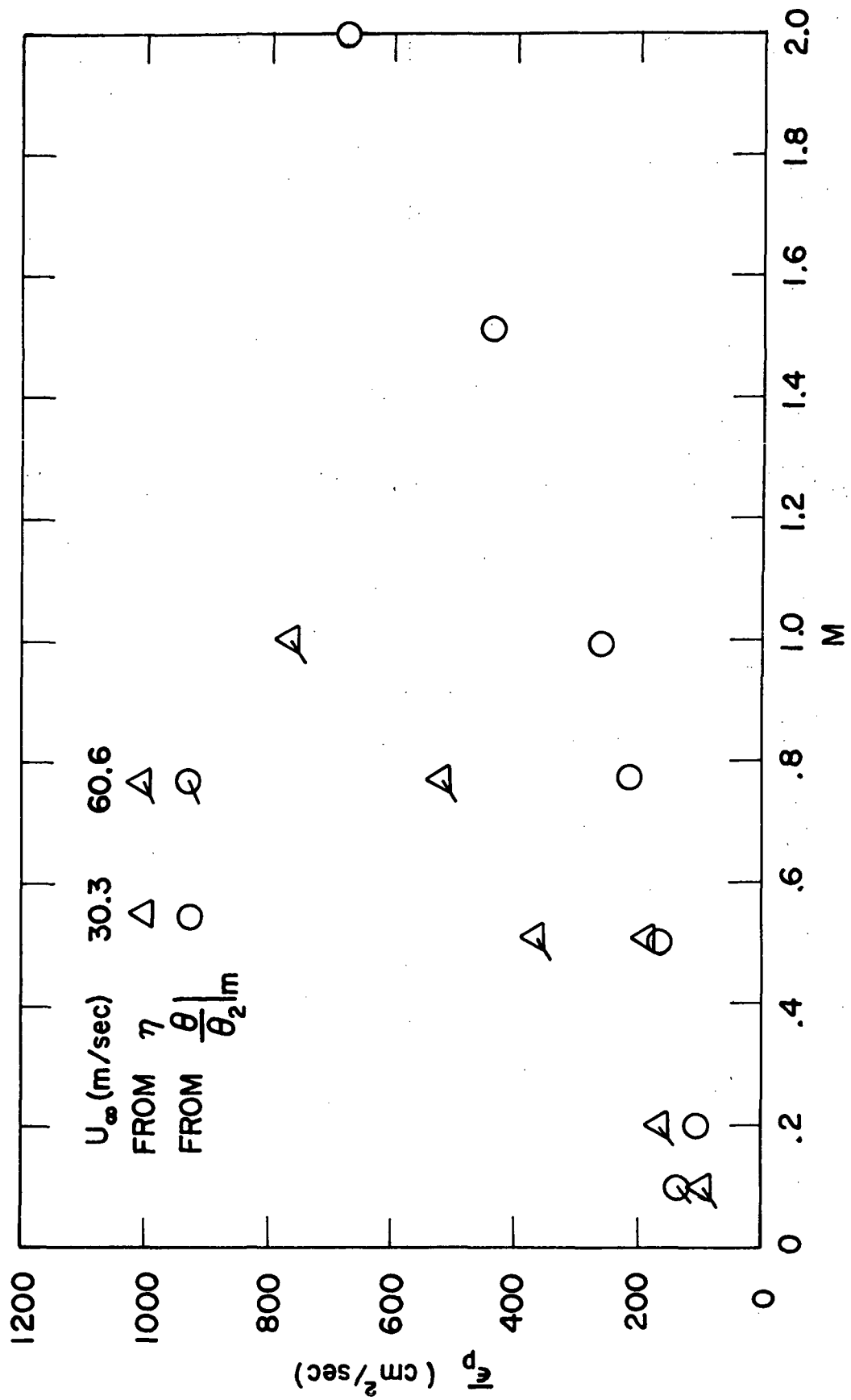Figure 3 - Average penetration of a jet injected normal to a crossflow

Figure 4 - Average effective turbulent diffusivity for a point source

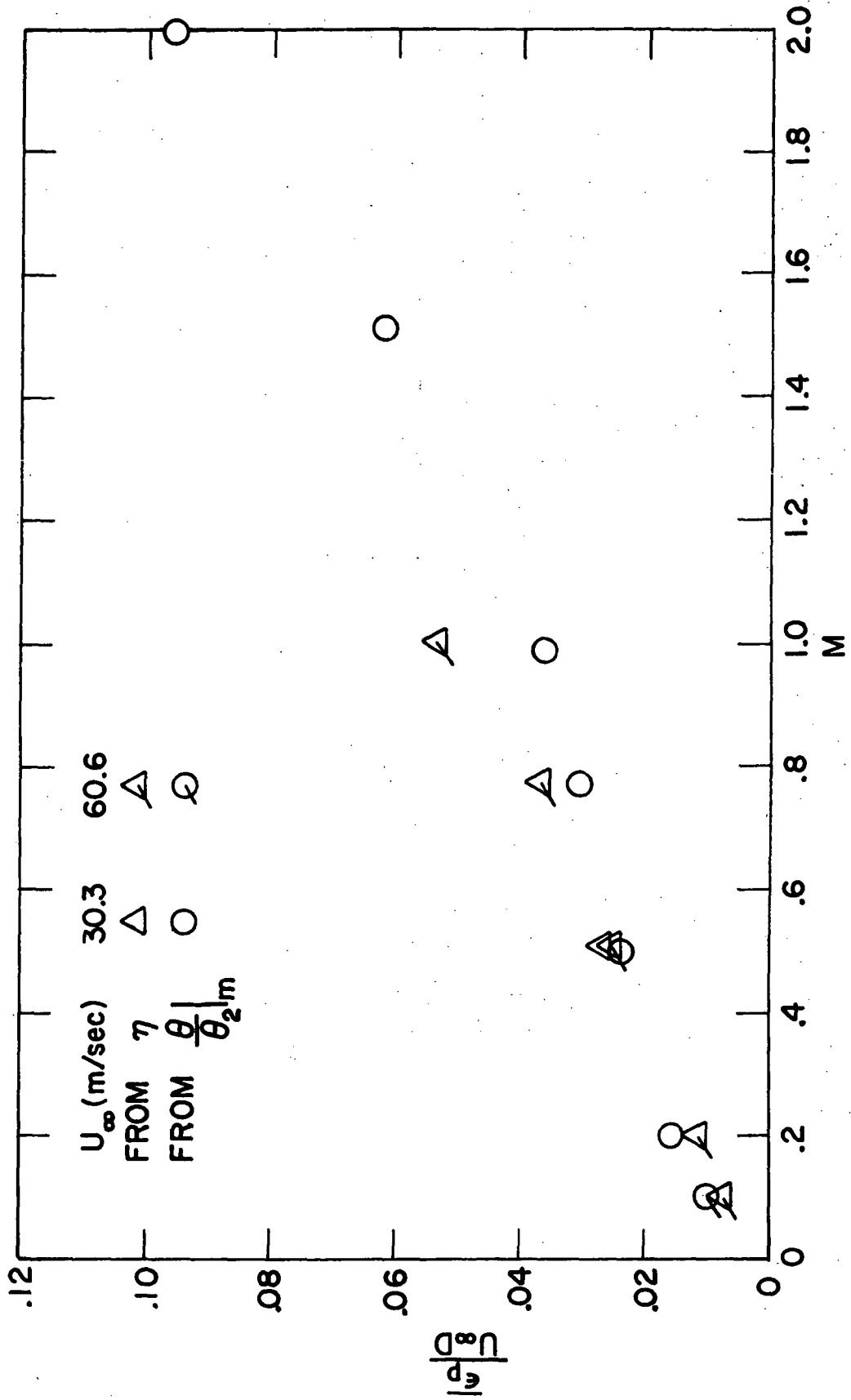Figure 5 – Dimensionless average effective turbulent diffusivity for a point source

Figure 6 - Comparison of temperature profiles predicted by point source model with experimental results

Figure 7 - Comparison of temperature profiles predicted by point source model with experimental results
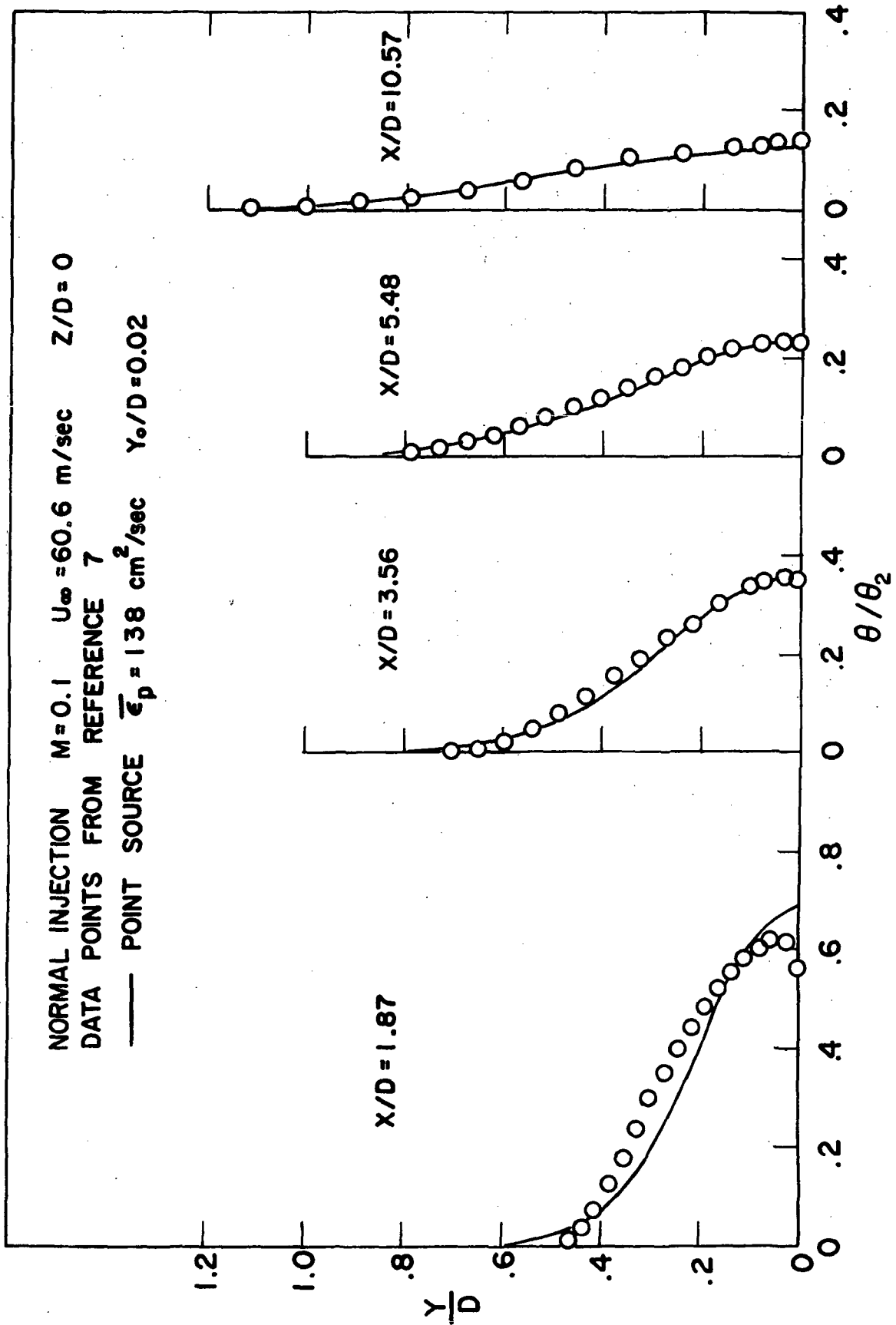
Figure 8 - Comparison of temperature profiles predicted by point source model with experimental results

Figure 9 - Comparison of temperature profiles predicted by point source model with experimental results

-30-

Figure 10 - Comparison of film cooling effectiveness predicted by point source model with experimental results

Figure 11 - Comparison of film cooling effectiveness predicted by point source model with experimental results

Figure 12 - Comparison of film cooling effectiveness predicted by point source model with experimental results
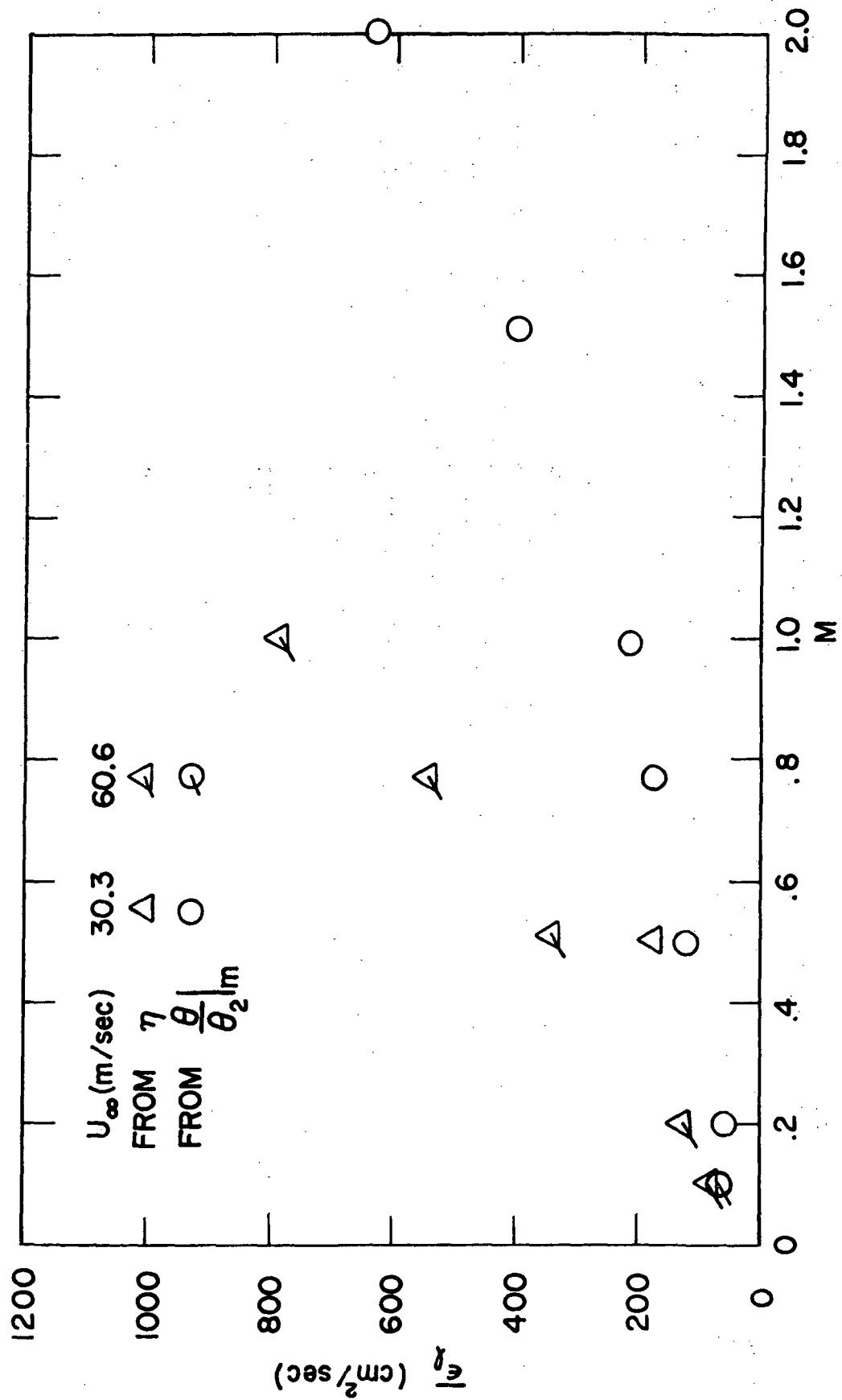
Figure 13 - Average effective turbulent diffusivity for a line source
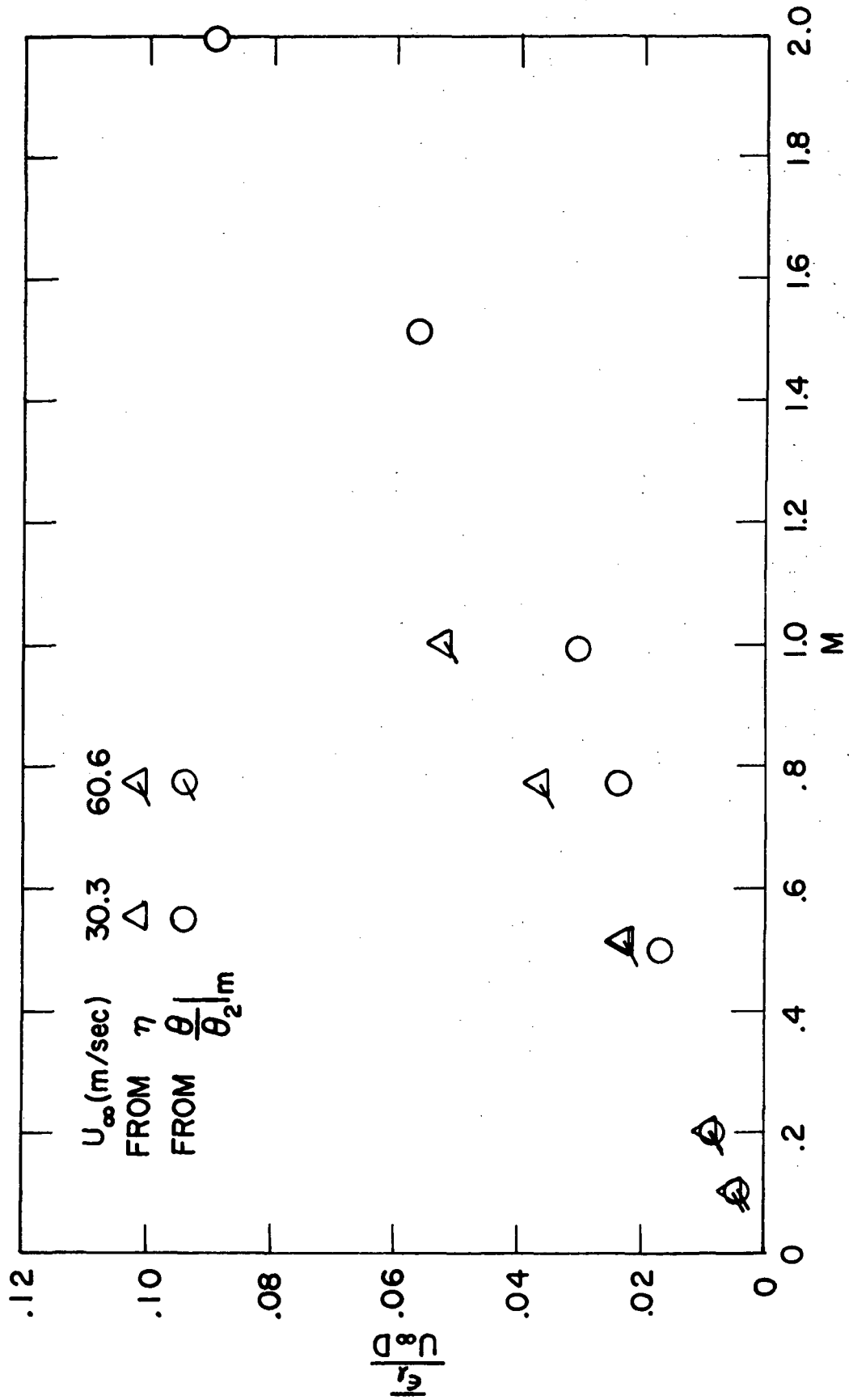
Figure 14 - Dimensionless average effective turbulent diffusivity for a line source

NORMAL INJECTION   M=0.10 U_∞=60.6 m/sec   Z/D = 0

DATA POINTS FROM   REFERENCE 7

—— LINE SOURCE $\bar{\epsilon_f}$ = 65 cm^2/sec Y_o/D =0.02

X/D=10.57

X/D=5.48

X/D=3.56

X/D=1.87
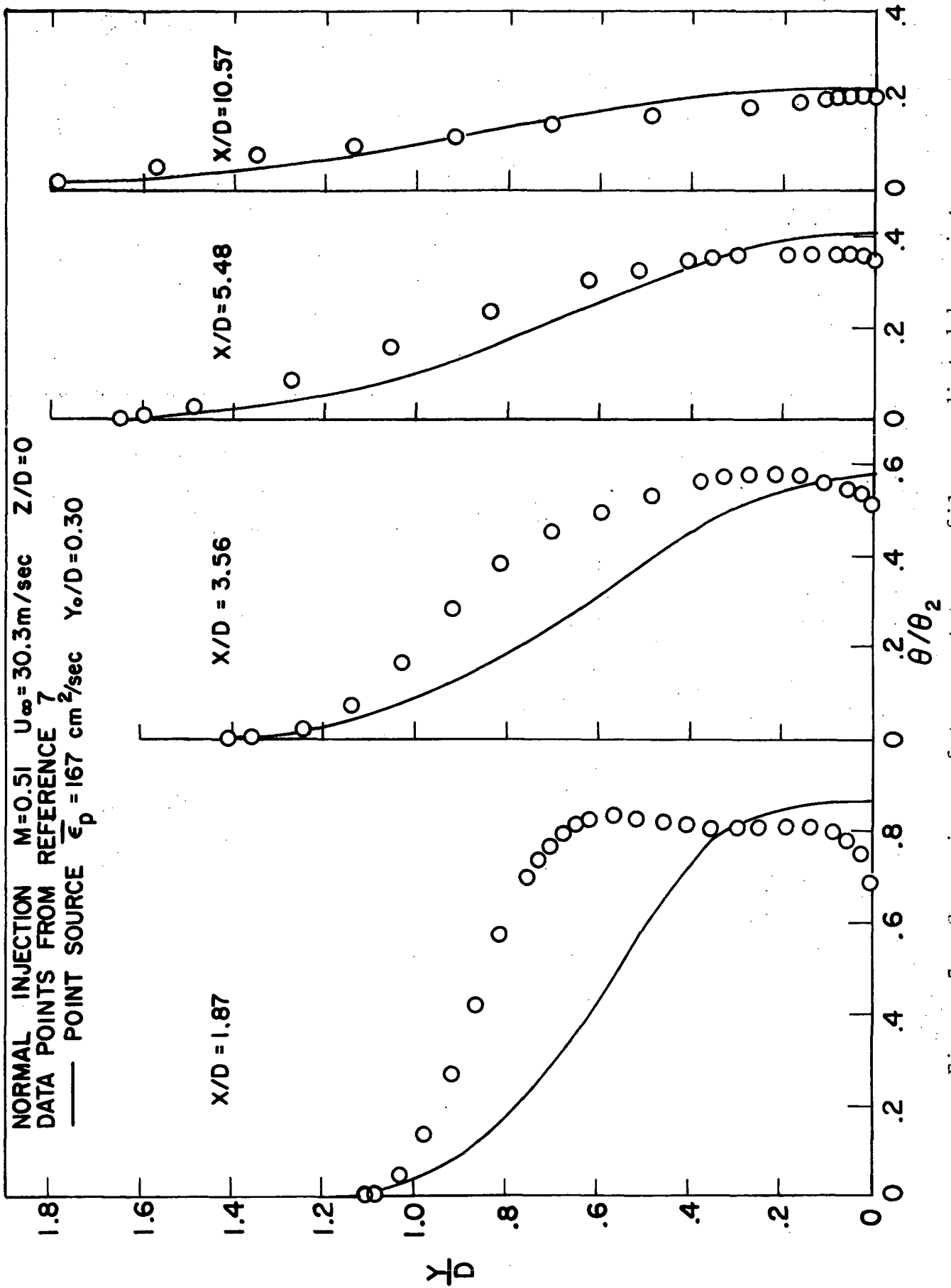
θ/θ_2

$\dfrac{Y}{D}$
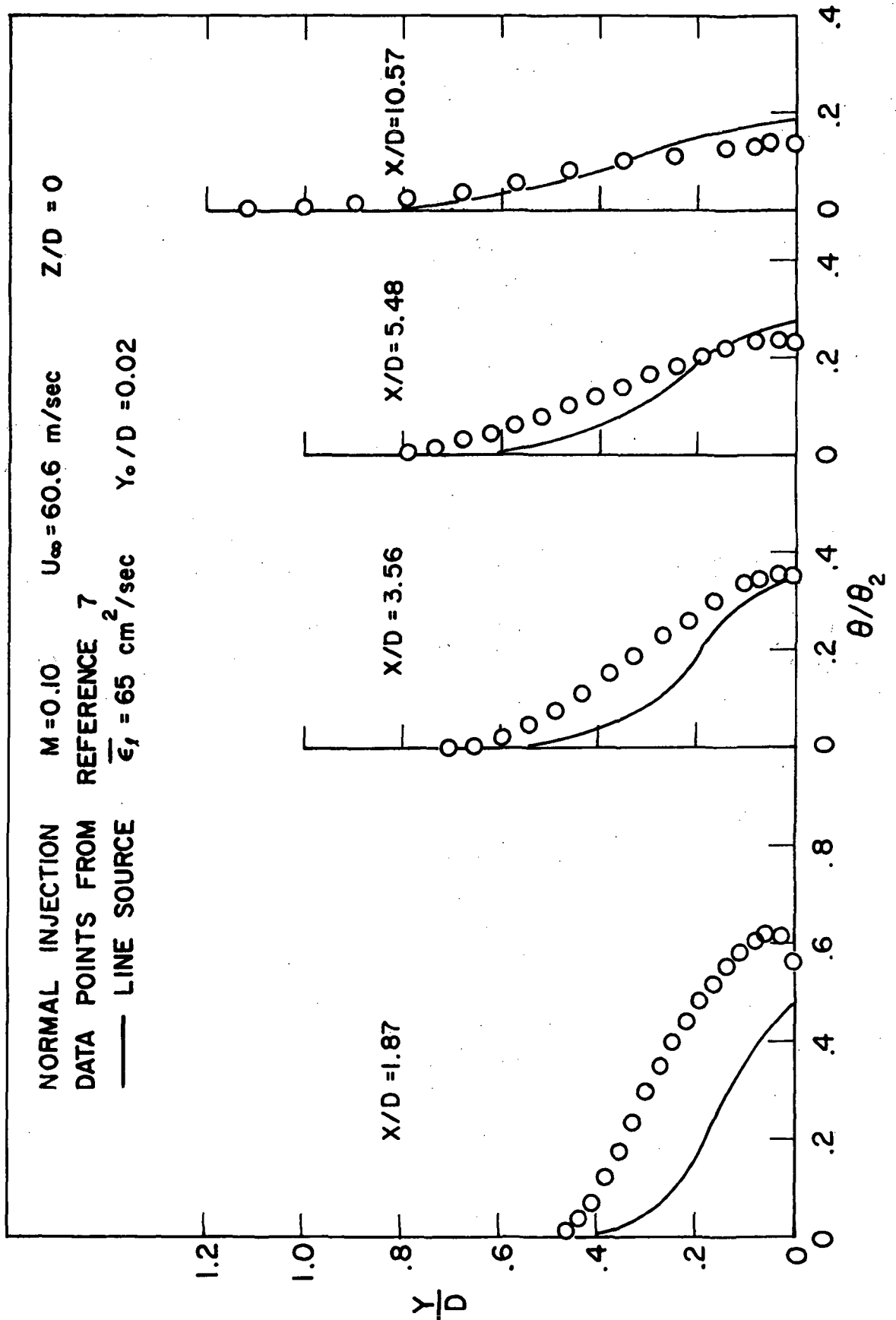
Figure 15   Comparison of temperature profiles predicted by line source
model with experimental results

-36-
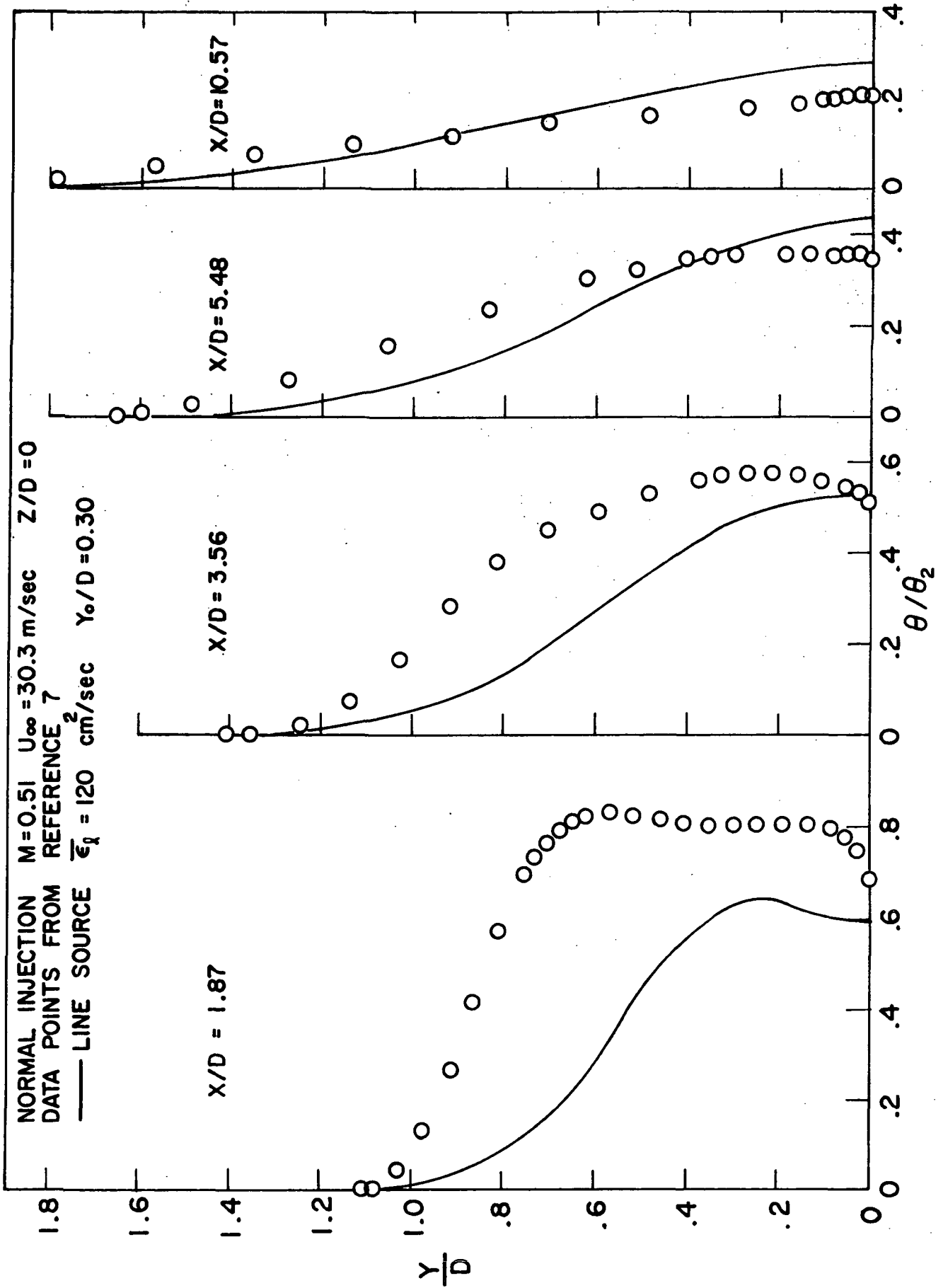
Figure 16 - Comparison of temperature profiles predicted by line source model with experimental results

Figure 17 - Comparison of temeprature profiles predicted by line source
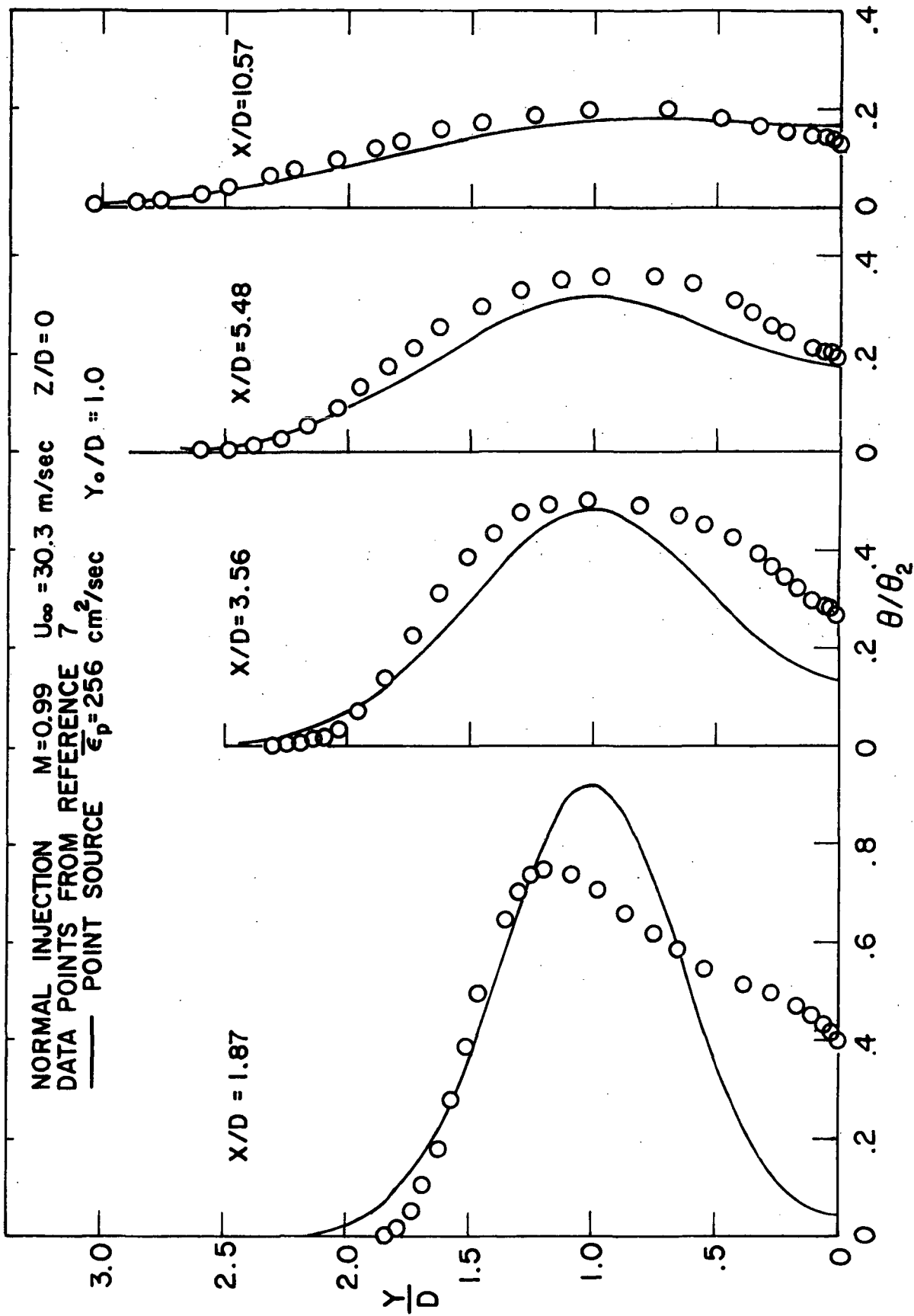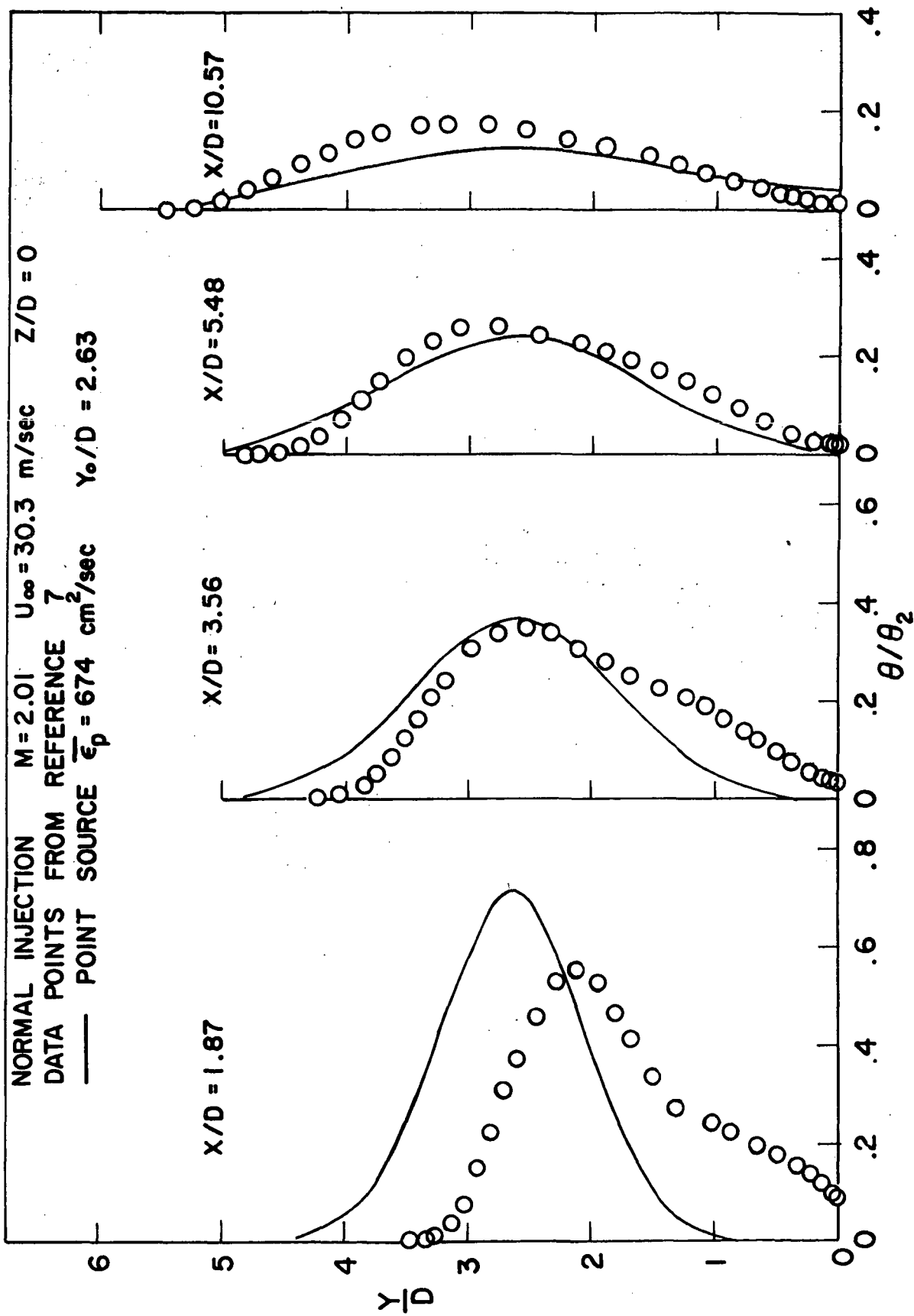model with experimental results

Figure 18 - Comparison of temperature profiles predicted by line source model with experimental results

Figure 19 - Comparison of film cooling effectiveness predicted by line
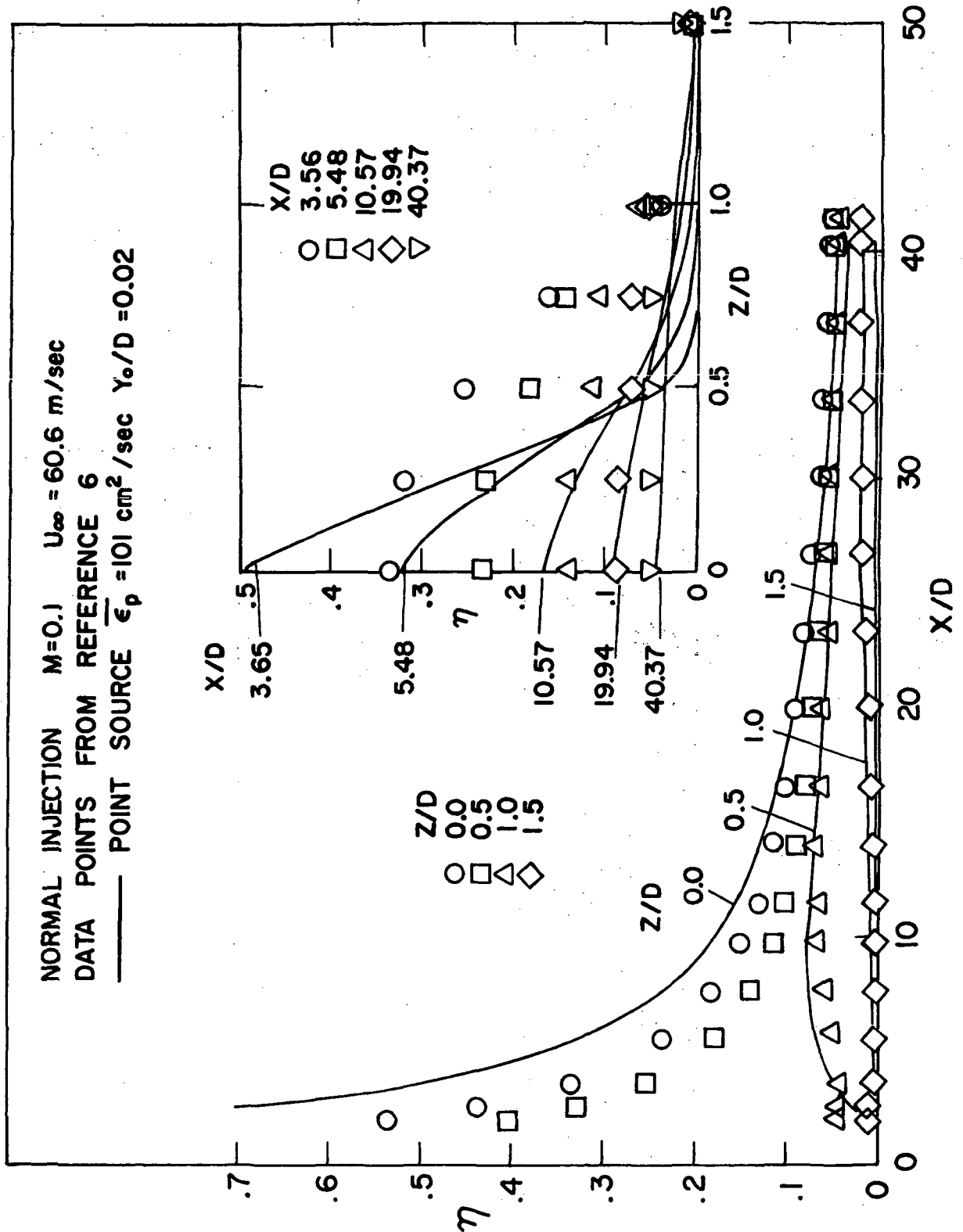source model with experimental results
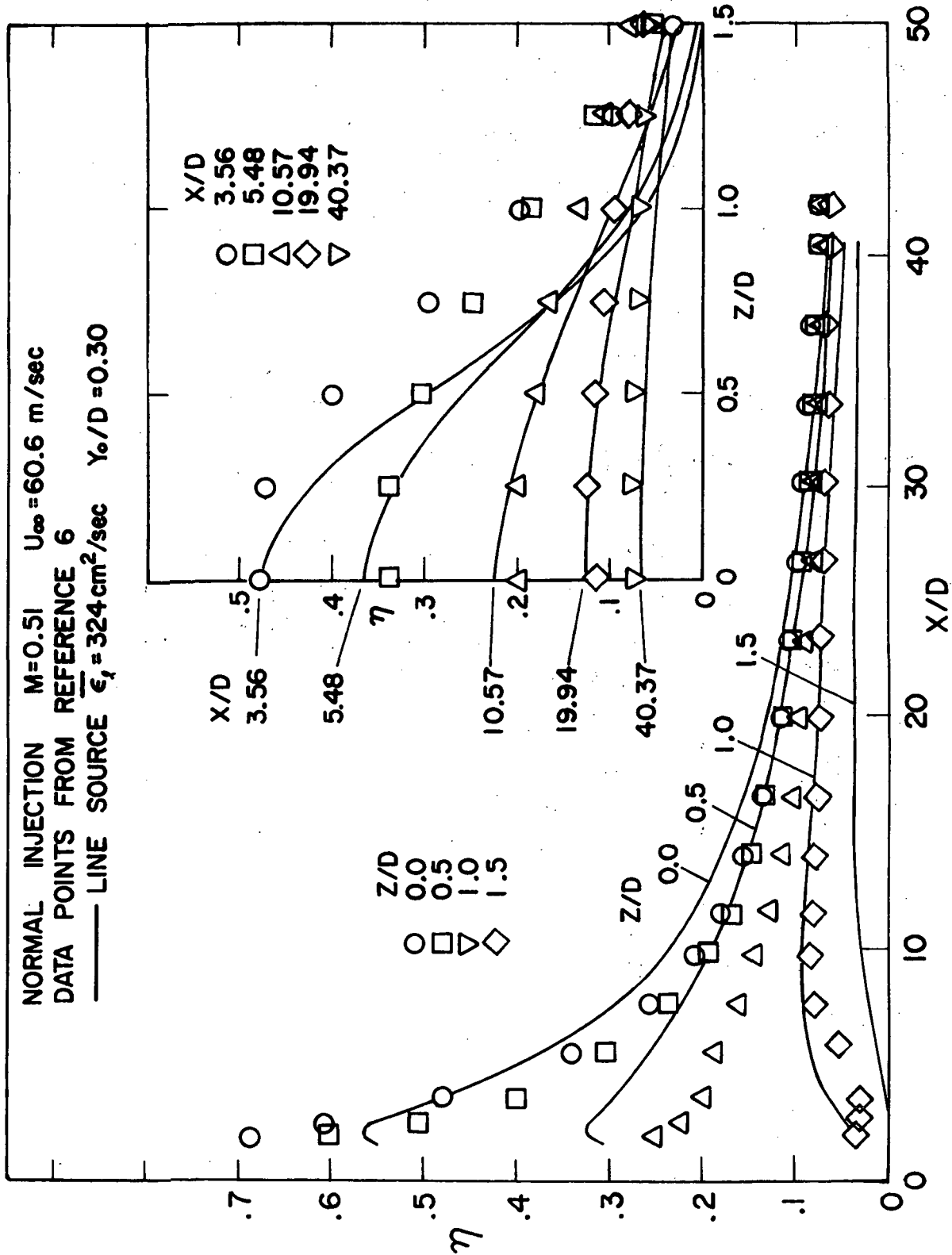
Figure 20 - Comparison of film cooling effectiveness predicted by line source model with experimental results
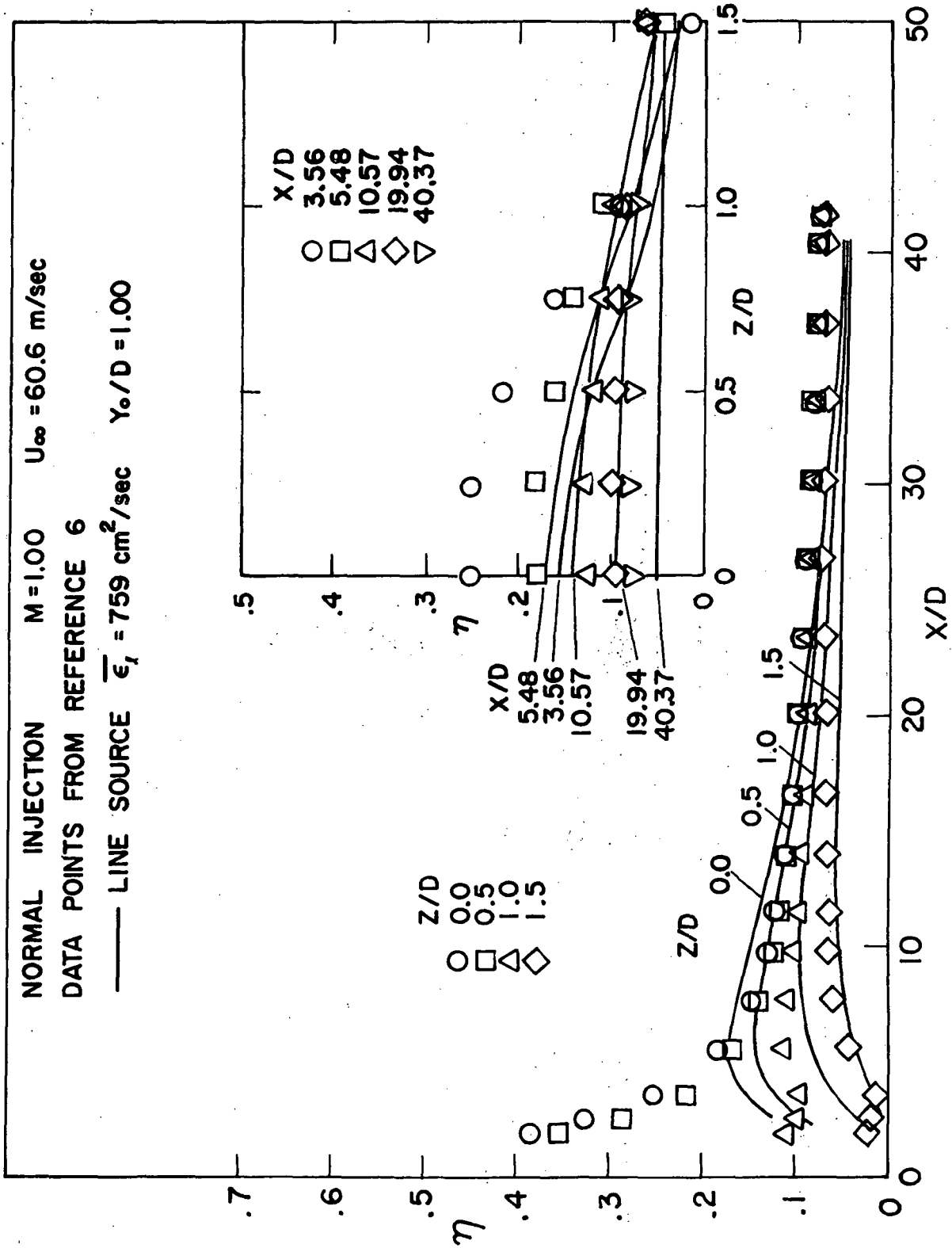
Figure 21 - Comparison of film cooling effectiveness predicted by line
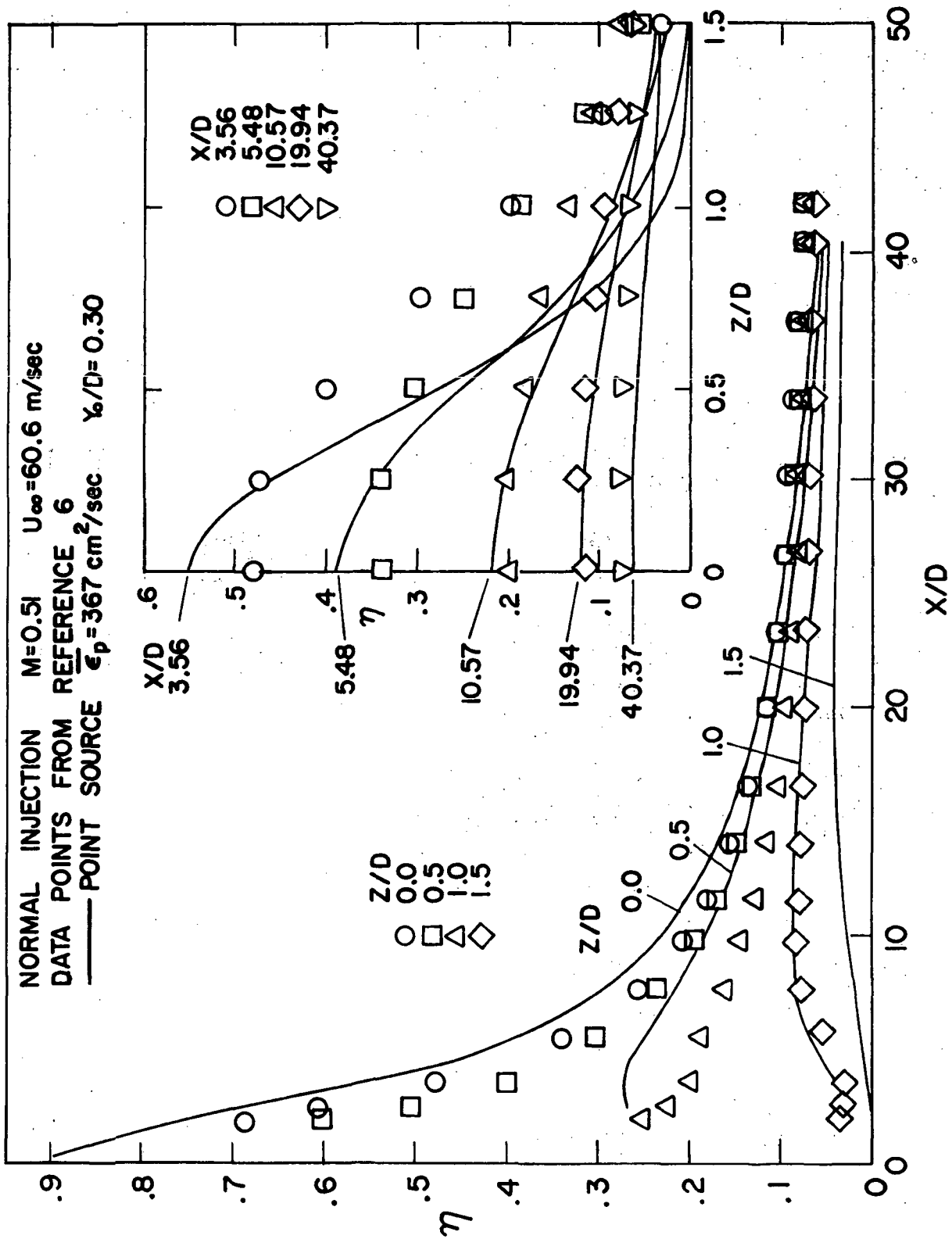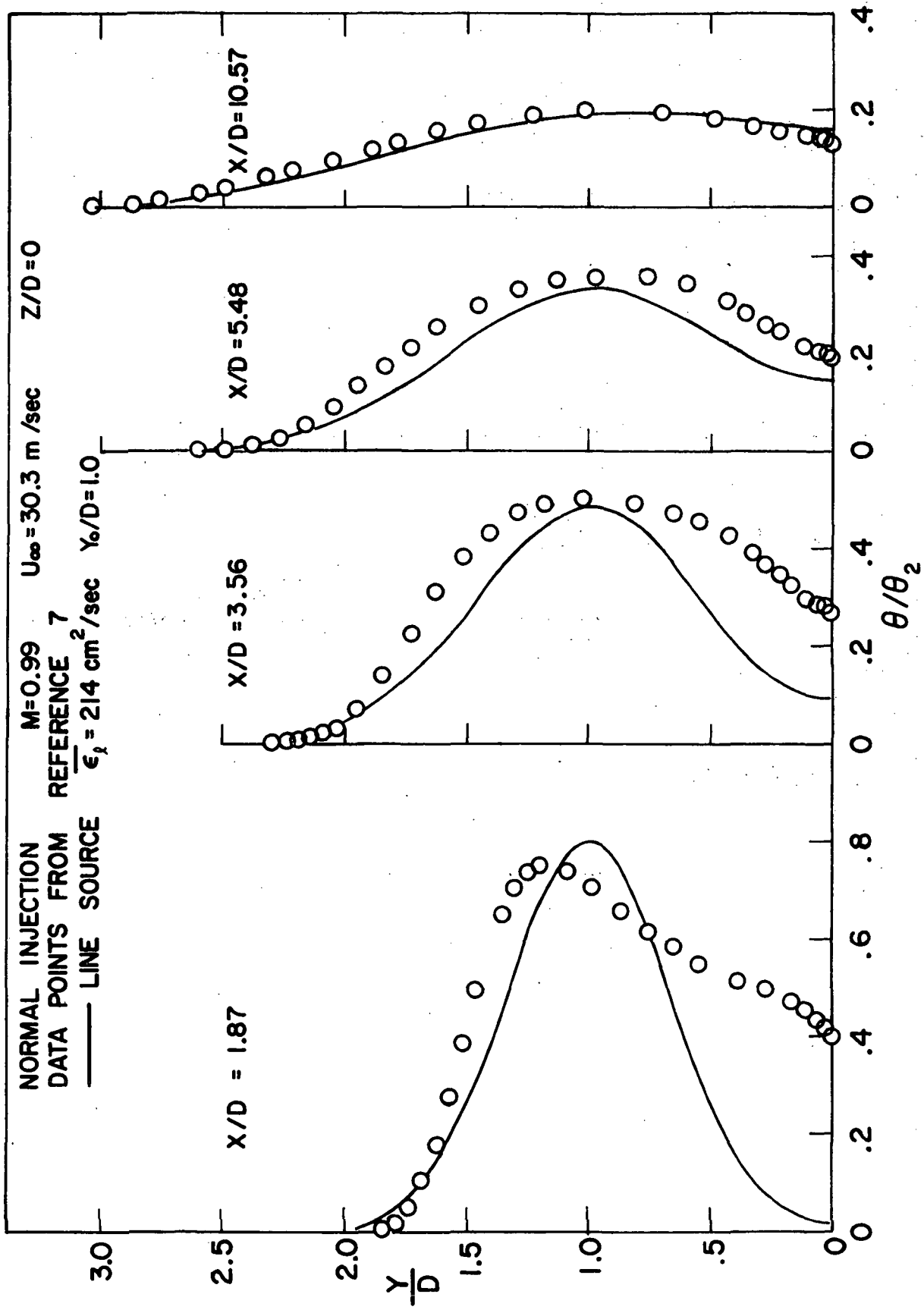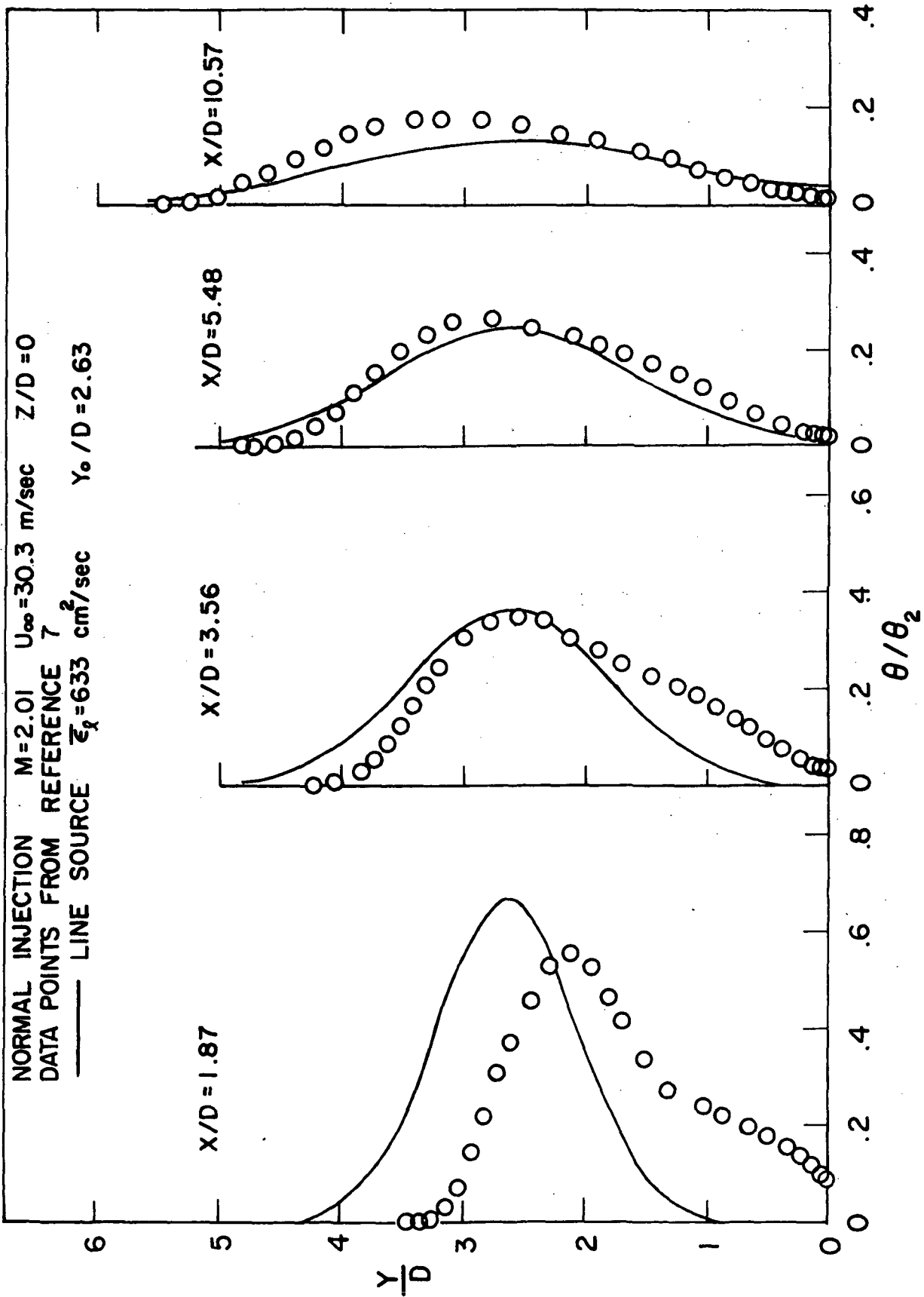source model with experimental results

| | NUMBER OF |
| ADDRESSEE | COPIES |

1. NASA Lewis Research Center
    21000 Brookpark Road   Mail
    Cleveland, Ohio 44135   Stop
    Attention: Aeronautics Procurement Section   77-3   1
                Reports Control Office   5-5   1
                Technology Utilization Office   3-19   1
                Library   60-3   2
                Fluid System Components Div.   5-3   1
                B. Lubarsky   3-3   1
                J. Howard Childs   60-4   1
                J. B. Esgar   60-4   1
                F. S. Stepka   60-6   10
                R. S. Colladay   60-6   1
                H. Ellerbrock   60-4   6
                J. Livingood   60-6   1

2. NASA Scientific & Technical Information Facility
    P.O. Box 33
    College Park, Maryland 20740
    Attention: NASA Representative RQT-2448   6

3. Dr. W. Kays
    Stanford University
    Stanford, California 94305   1

4. NASA Headquarters
    Washington, D.C. 20546
    Attention: N. F. Rekos (RLC)   1

5. Department of the Army
    U.S. Army Aviation Material Laboratory
    Fort Eustis, Va. 23604
    Attention: John White   1

6. Headquarters
    Wright-Patterson AFB, Ohio 45433
    Attention: Jack Richens   (AFAPL/APTC)   2

7. Air Force Office of Scientific Research
    Propulsion Research Division
    USAF Washington, D.C. 20025   1

8. Defense Documentation Center (DDC)
   Cameron Station
   5010 Duke Street
   Alexandria, Virginia 22314   1

9. NASA-Langley Research Center
   Langley Station
   Technical Library
   Hampton, Virginia 23365
   Attention: Mark R. Nichols   1
               John V. Becker   1

10. United Aircraft Corporation
    Pratt & Whitney Aircraft Division
    Florida Research & Development Center
    P.O. Box 2691
    West Palm Beach, Florida 33402
    Attention: R. A. Schmidtke   1

11. United Aircraft Corporation
    Pratt & Whitney Aircraft Division
    400 Main Street
    East Hartford, Connecticut 06108
    Attention: C. Andreini   2
                Library   1
                M. Suo   1

12. United Aircraft Research
    East Hartford, Connecticut
    Attention: Library   1

13. Allison Division of GMC
    Department 8894, Plant 8
    P.O. Box 894
    Indianapolis, Indiana 46206
    Attention: J. N. Barney   1
                C. E. Holbrook   1
                Library   1

14. Northern Research & Engineering Corporation
    219 Vassar Street
    Cambridge, Massachusetts
    Attention: K. Ginwala   1

15. General Electric Company
    Flight Propulsion Division
    Cincinnati, Ohio 45125
    Attention: J. W. McBride   N-44   1
                F. Burggraf   H-32   1
                S. N. Suciu   H-32   1
                Technical Information Center N-32   1

16. General Electric Company
    1000 Western Avenue
    West Lynn, Massachusetts 01905
    Attention: Dr. C. W. Smith--Library Bldg. 2-40M   1

17. Curtiss-Wright Corporation
    Wright Aeronautical Division
    Wood-Ridge, New Jersey 07075
    Attention: S. Lombardo   1

18. Air Research Manufacturing Company
    402 South 36th Street
    Phoenix, Arizona 85034
    Attention: Robert O. Bullock   1

19. Air Research Manufacturing Company
    9851 Sepulveda Boulevard
    Los Angeles, California 90009
    Attention: Fred Faulkner   1

20. AVCO Corporation
    Lycoming Division
    350 South Main Street
    Stratford, Connecticut 06497
    Attention: Claus W. Bolton   1
               Charles Kuintzle   1

21. Continental Aviation & Engineering Corporation
    12700 Kercheval
    Detroit, Michigan 48215
    Attention: Eli H. Benstein   1
               Howard C. Walch   1

22. International Harvester Company
    Solar Division - 2200 Pacific Highway
    San Diego, California 92112
    Attention: P. A. Pitt   1
               Mrs. L. Walper   1

23. George Derderian AIR 53662B
    Department of Navy
    Bureau of Navy
    Washington, D.C. 20360   1

24. The Boeing Company
    Commercial Airplane Division
    P.O. Box 3991
    Seattle, Washington 98124
    Attention: C. J. Schott   80-66   1

25. Acrojet-General Corporation
    Sacramento, California 95809
    Attention: M. S. Nylin   1
                Library   1
                William Heath   1

26. Newark College of Engineering
    323 High Street
    Newark, New Jersey 07102
    Attention: Dr. Peter Hrycak   1

27. Department of Mechanical Engineering
    Arizona State University
    Tempe, Arizona
    Attention: Dr. D. E. Metzger   1